Biogeosciences, 17, 2521–2536, 2020
https://doi.org/10.5194/bg-17-2521-2020

Biogeosciences Open Access EGU

Ice formation on lake surfaces in winter causes warm-season bias of lacustrine brGDGT temperature estimates

Jiantao Cao[1,2], Zhiguo Rao[3], Fuxi Shi[4], and Guodong Jia[1]

[1]State Key Laboratory of Marine Geology, Tongji University, Shanghai 200092, China
[2]Key Laboratory of Western China's Environmental Systems, Ministry of Education, College of Earth and Environmental Sciences, Lanzhou University, Lanzhou 730000, China
[3]College of Resources and Environmental Sciences, Hunan Normal University, Changsha 410081, China
[4]Jiangxi Provincial Key Laboratory of Silviculture, College of Forestry, Jiangxi Agricultural University, Nanchang 330045, China

Correspondence: Zhiguo Rao (raozhg@hunnu.edu.cn) and Guodong Jia (jiagd@tongji.edu.cn)

Received: 21 December 2019 – Discussion started: 4 February 2020
Revised: 14 April 2020 – Accepted: 15 April 2020 – Published: 12 May 2020

Abstract. It has been frequently found that lacustrine branched glycerol dialkyl glycerol tetraethers (brGDGT)-derived temperatures are warm-season-biased relative to measured mean annual air temperature (AT) in the middle to high latitudes, the mechanism of which, however, is not very clear. Here, we investigated the brGDGTs from catchment soils, suspended particulate matter (SPM) and surface sediments in different water depths in Gonghai Lake in northern China to explore this question. Our results showed that the brGDGT distribution in sediments resembled that in the SPM but differed from the surrounding soils, suggesting a substantial aquatic origin of the brGDGTs in the lake. Moreover, the increase in brGDGT content and decrease in methylation index with water depth in sediments suggested more contribution of aquatic brGDGTs produced from deep or bottom waters. Therefore, established lake-specific calibrations were applied to estimate local mean annual AT. As usual, the estimates were significantly higher than the measured mean annual AT. However, they were similar to (and thus actually reflected) the mean annual lake water temperature (LWT). Interestingly, the mean annual LWT is close to the measured mean warm-season AT, thus suggesting that the apparent warm-season bias of lacustrine brGDGT-derived temperatures could be caused by the discrepancy between AT and LWT. In our study region, ice forms at the lake surface during winter, leading to isolation of the underlying lake water from air and hence higher LWT than AT, while LWT basically follows AT during warm seasons when ice disappears. Therefore, we think that lacustrine brGDGTs actually reflected the mean annual LWT, which is higher than the mean annual AT in our study location. Since the decoupling between LWT and AT in winter due to ice formation is a universal physical phenomenon in the middle to high latitudes, we propose this phenomenon could be also the reason for the widely observed warm-season bias of brGDGT-derived temperatures in other seasonally surface ice-forming lakes, especially in shallow lakes.

1 Introduction

The branched glycerol dialkyl glycerol tetraethers (brGDGTs), including 0–2 cyclopentyl moieties (a–c) and four to six methyl groups (I–III) (Weijers et al., 2007a), are components of the cell membranes of microorganisms ubiquitously found in marine and continental environments and sensitive to ambient environmental conditions (Sinninghe Damsté et al., 2000; Weijers et al., 2006a; Schouten et al., 2013). The relative amounts of methyl groups and cyclopentyl moieties, expressed as methylation index (MBT or modified MBT′) and cyclization ratio (CBT) of brGDGTs in soil brGDGTs, have been suggested to reflect mean annual air temperature (AT) (Weijers et al., 2007a; Peterse et al., 2012). With improved analytical methods, a series of 6-methyl brGDGTs, previously co-eluted with 5-methyl brGDGTs, were identified (De Jonge et al., 2013), which

may introduce scatter in the original MBT′–CBT calibration for the mean annual AT (De Jonge et al., 2014). Thus, exclusion of the 6-methyl brGDGTs from the MBT′, i.e., the newly defined MBT'_{5ME}, results in improved calibrations (De Jonge et al., 2014; Wang et al., 2016, 2019). Calibrations using globally distributed surface soils for the MBT–CBT, MBT′–CBT or MBT'_{5ME} indices (Weijers et al., 2007a; Peterse et al., 2012; De Jonge et al., 2014) have been widely used for continental AT reconstruction (e.g., Weijers et al., 2007b; Niemann et al., 2012; Lu et al., 2019).

The brGDGTs in lake environments were initially thought to be derived from soil input (Hopmans et al., 2004; Blaga et al., 2009), allowing the mean annual AT to be reconstructed from lake sediments. However, when the soil-based calibrations are applied to the lake materials, the estimated temperatures are usually significantly lower than actual local AT (Tierney and Russell, 2009; Tierney et al., 2010; Blaga et al., 2010; Loomis et al., 2011, 2012; Pearson et al., 2011; Sun et al., 2011; Russell et al., 2018), suggesting an intricate brGDGT response to ambient temperature in aquatic environments. Later, more and more studies reveal that brGDGTs could be produced in situ in lake environments and differ significantly from soil-derived brGDGT distributions (Wang et al., 2012; Loomis et al., 2014; Naeher et al., 2014; Hu et al., 2015; Cao et al., 2017) and stable carbon isotope composition (Weber et al., 2015, 2018). The findings of intact polar lipid of brGDGTs, indicative of fresh microbial products, in lake water suspended particulate matter (SPM) and surface sediments (Tierney et al., 2012; Schoon et al., 2013; Buckles et al., 2014a; Qian et al., 2019) further confirm the in situ production of brGDGTs. Nevertheless, the brGDGT distribution in lake surface sediments has still been found to be strongly correlated with AT. Subsequently, quantitative lacustrine-specific calibrations for AT have been established at regional and global scales (Tierney et al., 2010; Pearson et al., 2011; Sun et al., 2011; Loomis et al., 2012; Shanahan et al., 2013; Foster et al., 2016; Dang et al., 2018; Russell et al., 2018), which have been widely used for AT reconstruction. These lacustrine-specific calibrations may reflect mean annual AT well in low-latitude regions (Tierney et al., 2010; Loomis et al., 2012), such as in Lake Huguang (21°09′ N, 110°17′ E) in southern China (Hu et al., 2015), Lake Donghu (30°54′ N, 114°41′ E) in central China (Qian et al., 2019) and Lake Towuli (2°30′ S, 121° E) on the island of Sulawesi (Tierney and Russell, 2009). However, they usually yield estimates biased to the warm (summer) seasons in middle- and high-latitude regions (Shanahan et al., 2013; Foster et al., 2016; Dang et al., 2018), such as in Lake Qinghai (36°54′ N, 100°01′ E) on the northeastern Tibetan Plateau (Wang et al., 2012), in Lower King Pond (44°25′ N, 72°26′ W) in temperate northern Vermont, USA (Loomis et al., 2014), and in the Arctic lakes (Peterse et al., 2014). The warm-biased temperature estimates in the middle- and high-latitude lakes have been postulated to be caused by the higher brGDGT production during warm seasons (e.g., Pearson et al., 2011; Shanahan et al., 2013).

The brGDGT-producing bacteria in soils could be metabolically active, hence producing abundant brGDGTs in warm and humid seasons, but they are suppressed in cold and/or dry environments (Deng et al., 2016; De Jonge et al., 2014; Naafs et al., 2017). However, it is presently unclear whether the brGDGTs in lacustrine sediments are mainly produced during the warm season. Investigations into lake water SPM reveal that a higher concentration of brGDGTs in the water column may occur in different seasons, e.g., in winter in Lake Lucerne in central Switzerland (Blaga et al., 2011), Lake Challa in tropical Africa (Buckles et al., 2014a), and Lake Huguang in subtropical southern China (Hu et al., 2016); in spring and autumn in Lower King Pond in temperate northern Vermont, USA (Loomis et al., 2014); and in the warm season in Lake Donghu in central China (Qian et al., 2019). Moreover, the contribution of the aquatic brGDGTs to the sediments is quantitatively unknown and likely minor considering that brGDGT producers favor anoxic conditions (Weijers et al., 2006b; Weber et al., 2018) that usually prevail in bottom water and sediments, which may discount the application of SPM-derived findings to the sedimentary brGDGTs.

In fact, brGDGT-based temperature indices should directly record lake water temperature (LWT), rather than AT, if the brGDGTs in lake sediments are solely or mainly sourced from the lake environments (Tierney et al., 2010; Loomis et al., 2014). Thus, the mean annual AT estimate based on lake sedimentary brGDGTs is valid only when LWT is tightly coupled with AT. However, the relationship between LWT and AT is potentially complex in cold regions, as well as in deep lakes, and the coupling between the two is not always the case, which would hamper the application of brGDGTs for temperature estimates (Pearson et al., 2011; Loomis et al., 2014; Weber et al., 2018). In deep lakes, bottom water temperature usually decouples with AT, together with the predominant production of brGDGTs in deep water and sediments, causing weak correlations between brGDGT-derived temperature and AT (Weber et al., 2018). For shallow lakes, LWT does not always follow AT either, specifically in winter when AT is below the freezing point in cold regions, as has been shown in Lower King Pond (Loomis et al., 2014). However, the decoupling between LWT and AT has not been recognized as a key mechanism for the warm bias of brGDGT-derived temperatures observed widely in the middle- and high-latitude lakes, and seasonal production or deposition of brGDGTs is usually invoked as a cause (e.g., Pearson et al., 2011; Shanahan et al., 2013; Loomis et al., 2014). Here, we hypothesized that the decoupling between LWT and AT in middle- and high-latitude shallow lakes, rather than the warm-season production, could have caused the frequently observed warmer temperature estimates from the lacustrine brGDGTs. To test this hypothesis, we investigated Gonghai Lake (a shallow alpine lake) in northern China by collecting

SPM and surface sediments in different depths in the lake and soils in its catchment in a hot summer and a cold winter. We analyzed brGDGT distributions in these materials to determine the sources of brGDGTs in the lake and further discussed the possible reasons for the warm bias of brGDGT-estimated temperatures.

2 Materials and methods

2.1 Gonghai Lake

Gonghai Lake (38°54′ N, 112°14′ E, ca. 1860 m above sea level (a.s.l.); Fig. 1a and b) is located on a planation surface of the watershed between the Sangkan River and the Fen River at the northeastern margin of the Chinese Loess Plateau. The location is close to the northern boundary of the modern East Asian summer monsoon (EASM, Chen et al., 2008; Fig. 1a). The modern local climate is controlled mainly by the East Asian monsoon system, with a relatively warm and humid summer resulting from the prevailing EASM from the southeast and a relatively cold and arid winter under the prevailing East Asian winter monsoon (EAWM) from the northwest (Chen et al., 2013, 2015; Rao et al., 2016). The mean annual precipitation is ca. 482 mm, concentrated (75 %) between July and September (Chen et al., 2013). Its total surface area is ca. 0.36 km^2, and the maximum water depth is ca. 10 m. Based on a nearby weather station, the measured mean annual AT has been 4.3 °C for the past 30 years. The warm season lasts from May to September (Fig. 1c), when column stratification develops with an upper-bottom temperature difference > 1 °C. During the winter from November to March, ice forms on the lake surface and LWT under ice is vertically constant at ca. 4 °C, which is significantly higher than AT, which is much below the freezing point (Fig. 1c). From April to October, the ice disappears and LWT follows AT closely, demonstrating a coupling between them (Fig. 1c). The vegetation type of the planation surface belongs to transitional forest steppe, dominated by *Larix principis-rupprechtii*, *Pinus tabulaeformis* and *Populus davidiana* forest, *Hippophae rhamnoides* scrub, *Bothriochloa ischaemum* grassland and *Carex* spp. (Chen et al., 2013; Shen et al., 2018).

2.2 Sampling

In September 2017, five surface soil samples in the catchment and five surface sediment samples at different depths (1.0, 2.5, 5.5, 6.7 and 8.0 m) in Gonghai Lake were collected (Fig. 1b). At each soil sample site, we collected five to six subsamples (top 0–2 cm) within an area of ca. 100 m^2 with contrasting micro-topography or plant cover and then mixed them to represent a single sample. To avoid possible human disturbances, the soil sampling sites were distant from roads and buildings. All samples collected in the field were stored in a refrigeration container during transportation and then freeze-dried for > 48 h in the laboratory. Details of all the sampling sites, including locations, sample depth and vegetation type, are listed in Table 1.

In addition, we also collected two batches of SPM samples at water depths of 1, 3, 6 and 8 m by filtering 50 L water through a 0.7 µm Whatman GF/F filter on site in September 2017 and January 2018, respectively. SPM samples were also stored in a refrigeration container during transportation and then freeze-dried for > 48 h in the laboratory. At the same time as the SPM sampling, we measured water column parameters in the lake using a YSI water quality profiler.

2.3 Sample treatment and GDGT analysis

Freeze-dried soil and sediment samples were homogenized at room temperature and accurately weighed. Each freeze-dried filter with SPM attached was cut into small pieces using a sterilized scissor. Each sample of soil, sediment and SPM was placed in a 50 mL tube and then ultra-sonicated successively with dichloromethane / methanol (DCM / MeOH, 1 : 1, v/v) four times. After centrifugation and combination of all the extracts of a sample, an internal standard, synthesized C_{46} GDGT, was added with a known amount (Huguet et al., 2006). Subsequently, the total extracts were concentrated using a vacuum rotary evaporator. The non-polar and polar fractions in the extracts were separated via silica gel column chromatography, using pure *n*-hexane and DCM / MeOH (1 : 1, v/v), respectively. The polar fraction containing GDGTs was dried in a gentle flow of N_2, dissolved in *n*-hexane / ethyl acetate (EtOA) (84 : 16, v/v) and filtered through a 0.45 µm polytetrafluoroethylene filter before instrumental analysis. We performed GDGT analysis by high-performance liquid chromatography–atmospheric pressure chemical ionization–mass spectrometry (HPLC-APCI-MS; Agilent 1200 series 6460 QQQ). Following the method of Yang et al. (2015), the separation of 5- and 6-methyl brGDGTs was achieved using two silica columns in tandem (150 mm × 2.1 mm, 1.9 µm, Thermo Finnigan; USA) maintained at 40 °C. The following elution gradient was used: 84 / 16 *n*-hexane / EtOA (A–B) to 82 / 18 A–B from 5 to 65 min and then to 100 % B in 21 min, followed by 100 % B for 4 min to wash the column and then back to 84 / 16 A–B to equilibrate it for 30 min. The flow rate was 0.2 mL min^{-1}. The brGDGTs were ionized and detected with single ion monitoring (SIM) at m/z 1050, 1048, 1046, 1036, 1034, 1032, 1022, 1020, 1018 and 744. The brGDGTs were quantified by comparing peak area of each brGDGT compound with the C_{46} GDGT internal standard. Based on duplicate HPLC-MS analyses, the analytical errors of both the MBT'_{5ME} and MBT'_{6ME} index were ±0.01 units.

Table 1. Concentration of brGDGTs, MBT'_{5ME}, MBT'_{6ME} and estimated temperatures in catchment surface soils, sediments and water column SPM in Gonghai Lake.

Code of site	Latitude (N)	Longitude (E)	Vegetation type	Water depth (m)	IIIa″ (ng g^{-1} dw)	Total brGDGTs (ng g^{-1} dw)	MBT'_{5ME}	MBT'_{6ME}	MAAT[a] (°C)	MAAT[b] (°C)	MAAT[c] (°C)	MAAT[d] (°C)	Growth AT[e] (°C)
Surface soils in Gonghai catchment													
S1	38°54′37.343″	112°14′19.039″	grass		0	74.82	0.31	0.21	1.20	−2.90			
S2	38°54′28.750″	112°14′18.460″	grass		0	23.50	0.36	0.20	2.58	−1.21			
S3	38°54′23.098″	112°14′24.140″	shrub		0	22.00	0.35	0.33	2.40	−4.22			
S4	38°54′27.126″	112°14′36.827″	shrub		0	32.65	0.36	0.26	2.64	−2.15			
S5	38°54′38.174″	112°14′40.502″	grass		0	16.06	0.36	0.24	2.82	−1.61			
Gonghai surface sediments													
D1	38°54′36.357″	112°14′22.963″		1.00	1.46	42.03	0.29	0.22	0.70	−4.24	8.35	13.50	6.91
D2	38°54′35.903″	112°14′24.004″		2.50	1.59	33.95	0.27	0.24	−0.13	−4.79	7.50	11.91	7.33
D3	38°54′35.294″	112°14′25.109″		5.50	17.87	327.62	0.23	0.25	−1.19	−6.53	6.40	10.11	7.70
D4	38°54′34.499″	112°14′27.301″		6.70	25.53	374.29	0.24	0.27	−0.93	−7.32	6.67	10.57	8.00
D5	38°54′33.980″	112°14′28.453″		8.00	42.96	706.72	0.24	0.25	−0.95	−6.44	6.64	10.72	7.67
Gonghai SPM in Sep													
Water 1 m	38°54′33.980″	112°14′28.453″		1.00	0.29[f]	5.71[f]	0.28	0.32	0.24	−6.00	7.88	11.19	9.16
Water 3 m	38°54′33.980″	112°14′28.453″		3.00	0.36[f]	6.39[f]	0.27	0.28	−0.05	−5.46	7.57	10.86	8.25
Water 6 m	38°54′33.980″	112°14′28.453″		6.00	0.30[f]	6.22[f]	0.26	0.29	−0.35	−6.55	7.26	10.45	8.55
Water 8 m	38°54′33.980″	112°14′28.453″		8.00	0.49[f]	10.07[f]	0.23	0.24	−1.40	−6.79	6.18	10.60	7.31
Gonghai SPM in Jan													
Water 1 m	38°54′33.980″	112°14′28.453″		1.00	0.16[f]	2.88[f]	0.25	0.27	−0.75	−6.32	6.85	10.40	7.95
Water 3 m	38°54′33.980″	112°14′28.453″		3.00	0.36[f]	6.09[f]	0.26	0.26	−0.49	−5.57	7.12	11.02	7.77
Water 6 m	38°54′33.980″	112°14′28.453″		6.00	0.49[f]	8.05[f]	0.25	0.27	−0.65	−6.24	6.95	10.57	7.99
Water 8 m	38°54′33.980″	112°14′28.453″		8.00	0.22[f]	3.71[f]	0.24	0.28	−0.96	−6.89	6.63	10.20	8.24

MAAT represents mean annual air temperature. [a] Calculated according to Eq. (9). [b] Calculated according to Eq. (10). [c] and [d] Calculated according to Eqs. (16) and (17), respectively. [e] Calculated according to Eq. (15). [f] The unit for brGDGT concentration is nanograms per liter (ng L^{-1}).

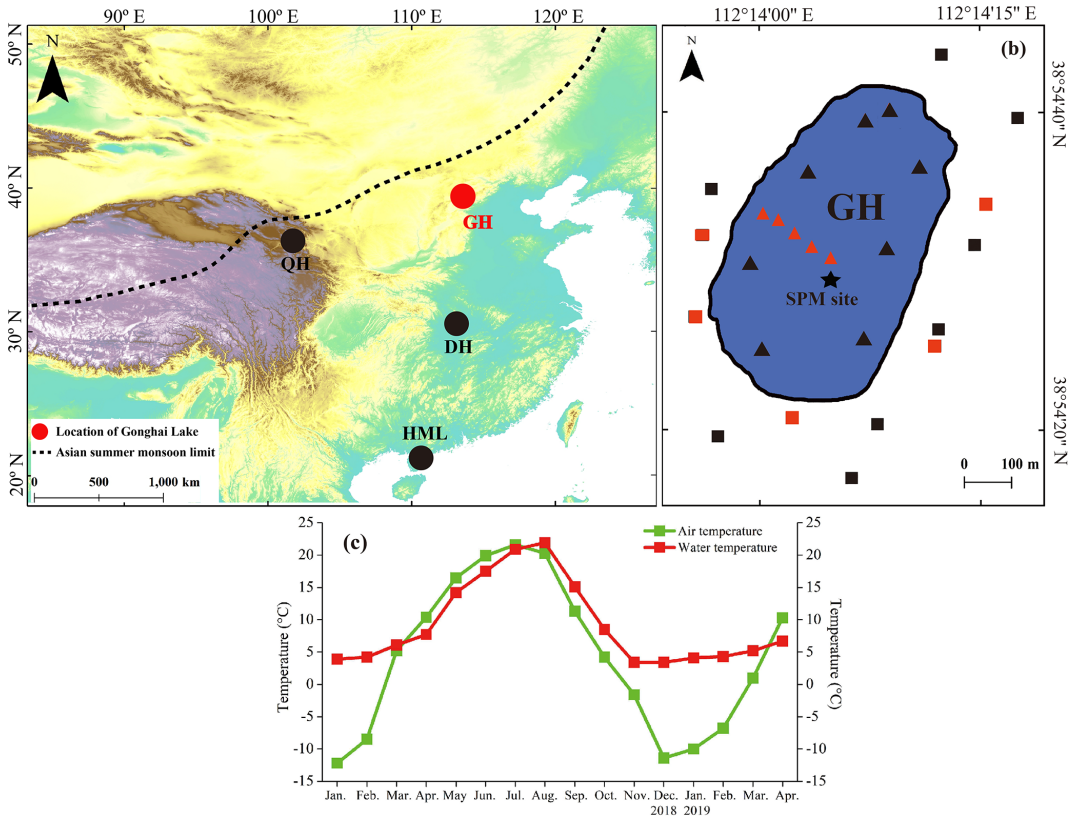

Figure 1. **(a)** Gonghai Lake (red circle), other referenced lakes (black circles) and the modern Asian summer monsoon limit (dashed line; Chen et al., 2008). **(b)** SPM from water column (black star), surface soils (red squares) and surface sediments (red triangles) in Gonghai Lake in this study; black squares and triangles represent the sample sites published in Cao et al. (2017). **(c)** Measured local air temperature (AT) and lake water temperature (LWT) during 2018–2019 (this study).

2.4 Calculation of GDGT-related proxies

The MBT'_{5ME} and MBT'_{6ME} index were calculated following Eqs. (1) and (2) following De Jonge et al. (2014):

$$MBT'_{5ME} = (Ia + Ib + Ic) / (Ia + Ib + Ic + IIa + IIb + IIc + IIIa), \quad (1)$$

$$MBT'_{6ME} = (Ia + Ib + Ic) / (Ia + Ib + Ic + IIa' + IIb' + IIc' + IIIa'). \quad (2)$$

The isomer ratio (IR) of 6-methyl was calculated following De Jonge et al. (2014). The ΣIIIa / ΣIIa ratio was calculated as in Martin et al. (2019), which is modified from Xiao et al. (2016). The weighted average number of cyclopentane for the tetra- and pentamethylated brGDGTs ($\#Rings_{tetra}$, $\#Rings_{penta\ 5ME}$ and $\#Rings_{penta\ 6ME}$) were calculated according to Sinninghe Damsté (2016):

$$IR_{6ME} = (IIa' + IIb' + IIc' + IIIa' + IIIb' + IIIc') / (IIa + IIa' + IIb + IIb' + IIc + IIc' + IIIa + IIIa' + IIIb + IIIb' + IIIc + IIIc'), \quad (3)$$

$$\Sigma IIIa / \Sigma IIa = (IIIa + IIIa' + IIIa'') / (IIa + IIa'), \quad (4)$$

$$\#Rings_{tetra} = (Ic \cdot 2 + Ib) / (Ia + Ib + Ic), \quad (5)$$

$$\#Rings_{penta\ 5ME} = (IIc \cdot 2 + IIb) / (IIa + IIb + IIc), \quad (6)$$

$$\#Rings_{penta\ 6ME} = (IIc' \cdot 2 + IIb') / (IIa' + IIb' + IIc'). \quad (7)$$

The Roman numerals represent different brGDGT homologues referred to in Yang et al. (2015) and Weber et al. (2015) (see Fig. S1 in the Supplement).

In this study, we used two silica columns in tandem and successfully separated 5- and 6-methyl brGDGTs. However, many previous brGDGT studies on lake materials used one cyano column that did not separate 5- and 6-methyl brGDGTs (e.g., Wang et al., 2012; Loomis et al., 2014; Hu et al., 2015, 2016; Cao et al., 2017). In order to facilitate comparison with previous studies, we reanalyzed the published brGDGT data without separation of 5- and 6-methyl brGDGTs in Gonghai Lake (Cao et al., 2017). For temperature estimations, we listed the Eqs. (8)–(17) used in this study in Table 2.

3 Results

3.1 Seasonal changes in environmental parameters

The AT in our study area ranged from −12.2 to 21.6 °C, below the freezing point in winter (November to February) and at 4.3 °C for the mean in the year 2018 (Fig. 1c). Surface LWT ranged from 3.4 to 21.9 °C (average 10.6 °C) and remained stable at ca. 4 °C in winter (Fig. 1c). In September 2017, water column stratification was weak, with temperatures ranging from 16.9 to 17.8 °C and exhibiting a gradual and slight decrease with depth (Fig. 2). In January 2018, the lake surface water was frozen and LWTs under ice were 4 °C at all depths (Fig. 2).

3.2 Concentration and distribution of brGDGTs

The brGDGTs were detected in all samples, and their total concentration ranged between 16 and 75 ng g^{-1} dry weight (dw) in surface soils from the Gonghai catchment, 42–707 ng g^{-1} dw in lake surface sediments, 5–10 ng L^{-1} in September and 3–8 ng L^{-1} in January in water SPM (Table 1 and Fig. 2). The average content of brGDGTs in lake surface sediments (291 ng g^{-1} dw) was significantly higher than in surface soils (31 ng g^{-1} dw) and exhibited a particularly increasing trend with water depth. In SPM, the average concentration of brGDGTs in the water column showed no significant difference between September and January ($t = 1.2$, $p = 0.26$), but there was a clearer trend of increase with depth in September than in January (Fig. 2). Notably, the compound IIIa″, which was regarded as typical for in situ produced lacustrine brGDGTs (Weber et al., 2015), was also identified in the Gonghai Lake sediments and SPM but not found in catchment soils (Table 1 and Fig. 3a). There was no significant difference in average concentrations of IIIa″ in the water column between September and January ($t = 0.62$, $p = 0.28$). The change patterns of IIIa″ with water depth in SPM and sediments were the same as those of the total brGDGTs (Table 1).

The brGDGTs in soils, sediments and SPM were dominated by brGDGT II and III series, with acyclic compounds dominant in every series (Fig. 3a). In comparison, the mean ΣIIIa / ΣIIa ratio value in sediments (1.14–1.52 range, 1.30 average) was higher than in SPM (0.84–1.11 range, 0.99 average) and soils (0.56–0.86 range, 0.70 average). In addition, 6-methyl brGDGTs dominated over 5-methyl brGDGTs in soils, exhibiting mean IR_{6ME} of 0.62, whereas the two isomers were similar in content in sediments ($IR_{6ME} = 0.47$–0.60 range, 0.51 average) and SPM ($IR_{6ME} = 0.45$–0.50 range, 0.48 average) (Fig. 3a).

3.3 Cyclization ratio and methylation index of brGDGTs

The $\#Rings_{tetra}$ values varied from 0.26 to 0.45 (0.36 average) in catchment soils, 0.37–0.43 (0.40 average) in September and 0.39–0.42 (0.40 average) in January in SPM, and 0.45–0.47 (0.45 average) in surface sediments (Fig. 3b). The $\#Rings_{penta\ 5ME}$ showed the same increasing trend as $\#Rings_{tetra}$ from soils to SPM and then to sediments (Fig. 3b). In contrast, $\#Rings_{penta\ 6ME}$ in soils was similar to that in sediments and SPM (Fig. 3b).

The MBT'_{5ME} values varied from 0.31 to 0.36 (0.35 average) in catchment soils, 0.23–0.29 (0.26 average) in surface sediments, 0.23–0.28 (0.26 average) in September and 0.24–0.26 (0.25 average) in January in SPM (Fig. 3b). Generally, the MBT'_{5ME} exhibited decreasing trends with water depth in surface sediments and SPM in September (Fig. 2). The MBT'_{6ME} values varied from 0.20 to 0.33 (0.25 average) in surface soils of the lake catchment, 0.22–0.27 (0.25 average) in surface sediments, 0.24–0.32 (0.28 average) in September and 0.26–0.28 (0.27 average) in January in SPM (Fig. 3b). The MBT'_{6ME} also decreased in SPM in September but increased in sediments with water depth. Both MBT'_{5ME} and MBT'_{6ME} changed less in SPM in January with water depth (Fig. 2).

4 Discussion

4.1 In situ production of brGDGTs in Gonghai Lake

Although brGDGTs have a strong potential to record temperature in lacustrine regions (Tierney et al., 2010; Pearson et al., 2011; Sun et al., 2011; Loomis et al., 2012; Dang et al., 2018; Russell et al., 2018), the sources of brGDGTs in lake sediments should be carefully identified. There are two potential sources, including allochthonous input from soil and autochthonous production in lake water and/or surface sediments, which can be distinguished through comparison of brGDGT distribution between surface sediments and soils (Tierney and Russell, 2009; Loomis et al., 2011; Wang et al., 2012; Hu et al., 2015; Sinninghe Damsté, 2016).

In Gonghai Lake, the average content of brGDGTs in surface sediments was significantly higher than that in surface soils (Table 1). Moreover, they exhibited a clearly increasing trend with water depth, suggesting a possible autochthonous contribution, even though soil brGDGTs input cannot be ignored. Moreover, the brGDGT distribution in surface sediments was similar to that of SPM but quite different from that of soils (Fig. 3a). Several lines of evidence indicate a substantial in situ production of brGDGTs in Gonghai Lake. (i) The presence of IIIa″ in Gonghai Lake sediments and SPM but the absence in the catchment soils may be a direct evidence of in situ production in the lake (Fig. 3a). A similar conclusion has been drawn in a Swiss mountain lake basin (Weber et al., 2015). (ii) In Gonghai Lake, the ΣIIIa / ΣIIa ratio in sediments (1.3 average) and SPM (0.99 average) were much higher than in catchment soils (0.7 average) (Fig. 3a). The values of ΣIIIa / ΣIIa > 0.92 have been regarded as evidence of aquatic production in previous reports (Xiao et al., 2016;

Table 2. Calibrations for brGDGT-derived temperature proxies used in this study.

Calibrations	Eq. no.	References
For soils		
$\mathrm{MAAT} = 0.81 - 5.67 \cdot \mathrm{CBT} + 31.0 \cdot \mathrm{MBT}'$ ($n = 176$, $r^2 = 0.59$, RMSE = 5.0 °C)	(8)	Peterse et al. (2012)
$\mathrm{MAAT} = -8.57 + 31.45 \cdot \mathrm{MBT}'_{5\mathrm{ME}}$ ($n = 222$, $r^2 = 0.66$, RMSE = 4.8 °C)	(9)	De Jonge et al. (2014)
$\mathrm{MAAT}^{a} = 27.63 \cdot \mathrm{Index\ 1} - 5.72$ ($n = 148$, $r^2 = 0.75$, RMSE = 2.5 °C)	(10)	Wang et al. (2016)
For sediments		
$\mathrm{MAAT} = 6.803 - 7.062 \cdot \mathrm{CBT} + 37.09 \cdot \mathrm{MBT}$ ($n = 139$, $r^2 = 0.62$, RMSE = 5.24 °C)	(11)	Global; Sun et al. (2011)
$\mathrm{MAAT} = 8.263 - 17.938 \cdot \mathrm{CBT} + 46.675 \cdot \mathrm{MBT}$ ($n = 24$, $r^2 = 0.52$, RMSE = 5.1 °C)	(12)	Regional; Sun et al. (2011)
$\mathrm{MAAT}^{b} = 50.47 - 74.18 \cdot f(\mathrm{IIIa}) - 31.60 \cdot f(\mathrm{IIa}) - 34.69 \cdot f(\mathrm{Ia})$ ($n = 46$, $r^2 = 0.94$, RMSE = 2.2 °C)	(13)	Tierney et al. (2010)
$\mathrm{MAAT} = 22.77 - 33.58 \cdot f(\mathrm{IIIa}) - 12.88 \cdot f(\mathrm{IIa}) - 418.53 \cdot f(\mathrm{IIc}) + 86.43 \cdot f(\mathrm{Ib})$ ($n = 111$, $r^2 = 0.94$, RMSE = 1.9 °C)	(14)	Loomis et al. (2012)
$\mathrm{Growth\ AT} = 21.39 \cdot \mathrm{MBT}'_{6\mathrm{ME}} + 2.27$ ($n = 39$, $r^2 = 0.75$, RMSE = 1.78 °C)	(15)	Dang et al. (2018)
$\mathrm{MAAT} = 23.81 - 31.02 \cdot f(\mathrm{IIIa}) - 41.91 \cdot f(\mathrm{IIb}) - 51.59 \cdot f(\mathrm{IIb}') - 24.70 \cdot f(\mathrm{IIa}) + 68.80 \cdot f(\mathrm{Ib})$ ($n = 65$, $r^2 = 0.94$, RMSE = 2.14 °C)	(16)	Russell et al. (2018)
$\mathrm{MAAT} = -1.21 + 32.42 \cdot \mathrm{MBT}'_{5\mathrm{ME}}$	(17)	Russell et al. (2018)

AT represents air temperature. MAAT represents mean annual air temperature. [a] $\mathrm{Index} = \log[(\mathrm{Ia} + \mathrm{Ib} + \mathrm{Ic} + \mathrm{IIa}' + \mathrm{IIIa}')/(\mathrm{Ic} + \mathrm{IIa} + \mathrm{IIc} + \mathrm{IIIa} + \mathrm{IIIa}')]$. [b] Fractional abundance of brGDGTs is a fraction of brGDGT Ia, IIa and IIIa only.

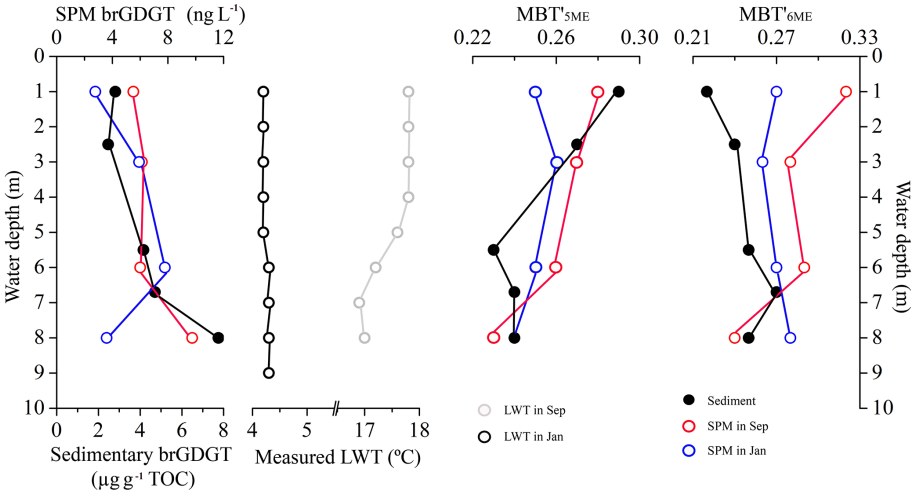

Figure 2. Depth profiles of water temperature, brGDGT concentrations, $\mathrm{MBT}'_{5\mathrm{ME}}$, $\mathrm{MBT}'_{6\mathrm{ME}}$ in water SPM from January and September, and sediments in Gonghai Lake.

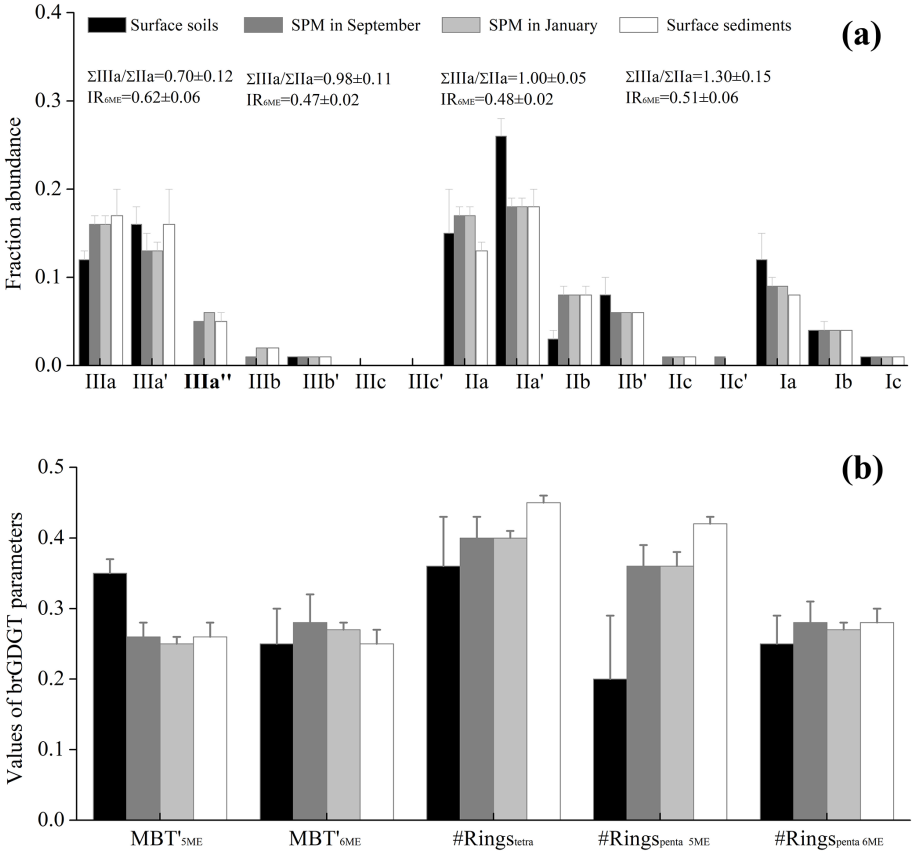

Figure 3. The brGDGT distribution in surface soils, water column (SPM) and surface sediments of Gonghai Lake. **(a)** Fractional abundance of brGDGTs. **(b)** Degree of methylation and cyclization of brGDGTs.

Martin et al., 2019; Zhang et al., 2020). (iii) The average values of IR_{6ME} in surface sediments and SPM were significantly lower than in catchment soils (Fig. 3a), suggesting at least some of 5-methyl brGDGTs in lake sediments and SPM were produced in situ. (iv) The cyclization ratio of brGDGTs has also been used to distinguish the aquatic production from soil input, although in previous studies this was applied to marine sediments (Sinninghe Damsté, 2016). In Gonghai Lake, $\#Rings_{tetra}$ and $\#Rings_{penta\ 5ME}$ were clearly higher in sediments than in catchment soils ($p < 0.05$ for $\#Rings_{tetra}$, $p < 0.01$ for $\#Rings_{penta\ 5ME}$), although $\#Rings_{penta\ 6ME}$ in sediments was similar to that in catchment soils ($p = 0.11$ for $\#Rings_{penta\ 6ME}$; Fig. 3b).

The in situ production of brGDGTs in Gonghai Lake is also evidenced by the discrepancies in reconstructed temperatures between soils and sediments or SPM. Based on the new global soil calibration of Eq. (9) and regional soil calibration of Eq. (10) for China, the brGDGT-derived AT in the Gonghai catchment soils ranged from 1.18 to 2.75 °C (average 2.33 ± 0.65 °C; Table 1) and from -4.22 to -1.21 °C (average -2.42 ± 1.19 °C; Table 1), respectively. Considering the ±4.8 °C uncertainty of the global calibration and ±2.5 °C of the regional calibration, the estimated temperatures from the global calibration are much close to the mean annual AT of 4.3 °C, thereby reflecting mean annual AT well in our study lake catchment. Following this, the global calibration Eq. (9) was applied to sediment and SPM data, yielding estimated temperatures -0.50 ± 0.78 °C in surface sediments and -0.55 ± 0.52 °C in SPM and hence are much lower than those from surface soils (2.33 ± 0.65 °C; Table 1). Similarly, temperature underestimation using soil-derived calibration has been widely reported in many modern lake sediments (e.g., Tierney et al., 2010; Loomis et al., 2012; Pearson et al., 2011; Russell et al., 2018), which has been attributed to in situ production of brGDGTs in the lakes.

4.2 Lacustrine brGDGT-derived ATs are warm-season-biased (average monthly temperature > 0 °C)

The suggested in situ production of brGDGTs prompted us to use lake-specific temperature calibrations (Tierney et al., 2010; Pearson et al., 2011; Sun et al., 2011; Loomis et al., 2012; Dang et al., 2018; Russell et al., 2018) to reconstruct AT, although the relative contributions of aquatic vs. soil-derived brGDGTs were not differentiated quantitatively.

Here, we applied four equations, Eqs. (11) and (15)–(17) in Table 2, to our sedimentary brGDGT data.

As shown in Fig. 4a, the reconstructed temperatures using different equations are > 6.4 °C. Despite discrepancies in the temperature values between calibrations, they are comparable considering the uncertainty of each calibration. A prominent feature of the reconstructed temperature is that it (especially in the shallower sediments) is well above the annual mean AT but more close to the mean warm-season AT (average monthly temperature > 0 °C). This feature is consistent with numerous studies proposing that lacustrine brGDGT-derived ATs are warm-season-biased (Shanahan et al., 2013; Peterse et al., 2014; Dang et al., 2018).

Many previous brGDGT instrumental analyses of lake materials used one cyano column that did not separate 5- and 6-methyl brGDGTs. Using the data published in the same lake from Cao et al. (2017), we recalculated temperature using different calibrations. The results showed that the absolute temperature estimates were all significantly warmer than the mean annual AT (Table 3), with the temperature offsets varying from 4 to 10 °C, which cannot be fully explained by the uncertainty of each calibration. Therefore, it appears that sedimentary brGDGT-derived temperature is warm-season-biased in Gonghai Lake irrespective of whether or not 5- and 6-methyl brGDGTs are separated.

Moreover, we found the warm-season bias of reconstructed AT is increasingly apparent with the increase in latitude. Here, five lakes, Lower King Pond (Loomis et al., 2014), Qinghai Lake (Wang et al., 2012), Lake Donghu (Qian et al., 2019), Lake Huguang (Hu et al., 2015, 2016) and Lake Towuli (Tierney and Russell, 2009), were selected to be compared as an example. These lakes are located in different regions spanning a relatively large environmental gradient, and, more importantly, brGDGT data from both the lake surface sediments and the surrounding soils are available. We recalculated temperatures from published data of brGDGTs from these lakes (Fig. 5) by applying the calibration of global soils (Eq. 8; Peterse et al., 2012) to the surrounding soils and the calibration of lake surface sediments (Eq. 11; Sun et al., 2011) to the lake sediments. As shown in Fig. 5a, the brGDGT-inferred temperatures in catchment soils are similar to local mean annual ATs. In contrast, the brGDGT-inferred temperatures in lake sediments are similar to the local mean annual ATs only in low-latitude lakes, whereas they increasingly become higher than the local mean annual ATs toward higher latitudes (Fig. 5b). In comparison, the brGDGT-inferred temperatures are close to the local mean ATs in the warm season (average monthly mean AT > 0 °C) in all of these lakes (Fig. 5c). Besides the above discussed lakes, some investigations have also pointed out that brGDGT-inferred temperatures are higher than mean annual AT and close to warm-season AT or summer AT in middle- and high-latitude lakes (Shanahan et al., 2013; Peterse et al., 2014; Foster et al., 2016; Dang et al., 2018), whereas they are close to (or lower than) mean annual AT in low-latitude lakes

Table 3. Comparison of measured air temperature, brGDGT-derived temperature from catchment soils and brGDGT-derived temperature from sediments in different lake basins.

Name	Latitude	Longitude	Depth	MAAT	Mean warm-season AT (°C)	Mean annual LWT (°C)	Surface soils MAAT[a] (°C)	Surface sediments MAAT[b] (°C)	Surface sediments MAAT[c] (°C)	Surface sediments MAAT[d] (°C)	References MAAT[e] (°C)	
			(m)	(°C)								
Gonghai Lake	38°54′ N	112°14′ E	9	4.3	12.1	10.6	3.96 ± 1.46	10.74 ± 0.33	9.70 ± 0.71	10.86 ± 1.33	7.93 ± 1.46	Cao et al. (2017)
Lake Towuti	2.5° S	121° E	200	24	24	–	22.52 ± 2.61	26.62 ± 1.10	29.13 ± 1.86	–	–	Tierney and Russell. (2009)
Lake Huguanyan	21°09′ N	110°17′ E	20	23.2	23.2	24.8	23.80 ± 1.39	25.11 ± 0.60	28.12 ± 0.90	26.47 ± 0.83	26.07 ± 0.73	Hu et al. (2015, 2016)
Lake Donghu	30°54′ N	114°41′ E	6	16	16	20	15.79 ± 4.37	19.74 ± 0.39	22.82 ± 0.51	25.75 ± 0.34	20.61 ± 0.71	Qian et al. (2019)
Lake Qinghai	36°54′ N	100°01′ E	27	0.65	7	–	3.38 ± 2.40	12.34 ± 0.87	9.92 ± 1.14	13.61 ± 1.49	8.80 ± 1.11	Wang et al. (2012)
Lower King Pond	44°25′ N	72°26′ W	8	6	11.3	11.6	11.50 ± 2.08	14.97 ± 0.42	14.9 ± 0.53	18.75 ± 0.64	15.76 ± 0.84	Loomis et al. (2014)

AT represents air temperature. MAAT represents mean annual air temperature. LWT represents lake water temperature. [a] Calculated according to Eq. (8). [b] and [c] Calculated according to Eqs. (11) and (12), respectively. [d] Calculated according to Eq. (13). [e] Calculated according to Eq. (14).

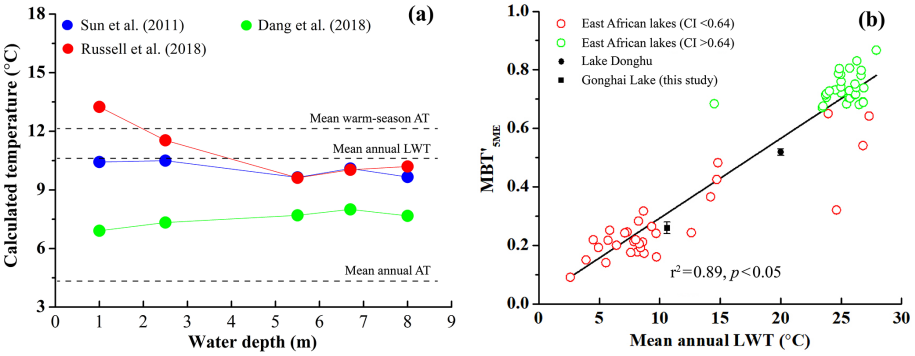

Figure 4. (a) The brGDGT-derived temperatures for sediments using lake calibrations Eqs. (11), (15) and (16) from Sun et al. (2011), Dang et al. (2018) and Russell et al. (2018), respectively. **(b)** The correlation between MBT'_{5ME} of sedimentary brGDGTs and mean annual lake water temperature (LWT). CI index represents Community Index (De Jonge et al., 2019). The brGDGT data of East African lakes, Lake Donghu and Gonghai Lake were sourced from Russell et al. (2018), Qian et al. (2019) and this study, respectively.

(Tierney et al., 2010; Loomis et al., 2012). Therefore, it is a global occurrence that sedimentary brGDGT-derived temperatures are warm-season-biased in lakes at cold regions.

4.3 Lacustrine brGDGTs reflect deep and bottom water temperature

Another feature of sedimentary brGDGT-derived ATs in our results is that there is a consistently decreasing trend of reconstructed temperature with depth using Eqs. (11), (15) and (16) (Fig. 4a), albeit less clear using Eq. (15). It is not understandable that AT is correlated with water depth. Interestingly, both MBT'_{5ME} and MBT'_{6ME} in SPM showed decreasing trends with water depth in September, similar to the water temperature profile of the month (Fig. 2). In January, the relatively unchanged MBT'_{5ME} and MBT'_{6ME} (< 0.02) also mirror the constant water temperature of the month (Fig. 2). Accordingly, we surmise that brGDGT-derived temperatures in sediments and SPM may actually reflect water temperature.

Although the MBT'_{5ME} and MBT'_{6ME} in SPM in the lake seem to reflect temperature changes in the water column to some extent, the differences of brGDGT-derived temperatures based on lake-specific calibrations between September and January (-0.93 to 1.21 °C) are much lower than the measured difference ($\sim$ 13 °C), independent of the calibration of Eqs. (15), (16) or (17) (Tables 1 and 2). In fact, similar results have been also reported in other lakes. For example, in Lower King Pond, the calculated seasonal temperature difference in surface water SPM was 5.4 °C, significantly smaller than the measured difference of about 28.3 °C (Loomis et al., 2014); in Lake Huguang, the calculated seasonal temperature difference was 8 °C, also significantly smaller than the measured difference about 16 °C (Hu et al., 2016). The reduced seasonal contrasts in SPM brGDGT-derived temperatures could result from the existence of "fossil" brGDGTs and sediment resuspension in the water column, which may lead to a long (e.g., multi-seasonal) residence time of SPM, although this is not exactly known (Loomis et al., 2014). The even smaller differences in MBT'_{5ME} and MBT'_{6ME} between sediments and SPM at deeper sites in our results (Fig. 2) suggest the impacts of sediment suspension on SPM. Such a scenario may lead to more fossil brGDGTs in SPM than those produced within a specific season or month, as evidenced by an observation showing that only a small proportion of intact polar lipid of brGDGTs, indicative of fresh brGDGTs, was detected in total brGDGTs in SPM in a shallow lake (Qian et al., 2019). Besides, several parameters, such as ΣIIIa / ΣIIa, IR_{6ME}, $\#Rings_{tetra}$ and $\#Rings_{penta}$ in SPM, were in-between the soil and sediment values, and we speculate terrestrial inputs may be a factor in the reduction of the seasonal changes of brGDGTs in SPM.

In addition to reflecting water temperature, the decease trend with depth in sedimentary brGDGT-derived temperature further suggests a controlling influence of deep and bottom water temperature. Similar occurrences have also been observed in Lower King Pond in temperate northern Vermont, USA, and Lake Biwa in central Japan, showing that the sedimentary brGDGT-derived temperatures decreased with water depth and covaried with mean annual LWT at depth (Ajioka et al., 2014; Loomis et al., 2014). Additionally, in Loch Lomond in the UK, the brGDGT-derived temperatures by different MBT–CBT lacustrine calibrations all decreased with water depth (Buckles et al., 2014b). Thus, a water-depth-related production of brGDGTs should be considered when interpreting brGDGT-derived temperatures, which will be discussed below.

A recent publication reported that changes in microbial community composition may be responsible for variations in the distribution of brGDGTs, causing the different responses of soil brGDGT temperature, as well as pH, under different temperature ranges (De Jonge et al., 2019). However, little is known about whether this idea is applicable to aquatic environments. According to De Jonge et al. (2019),

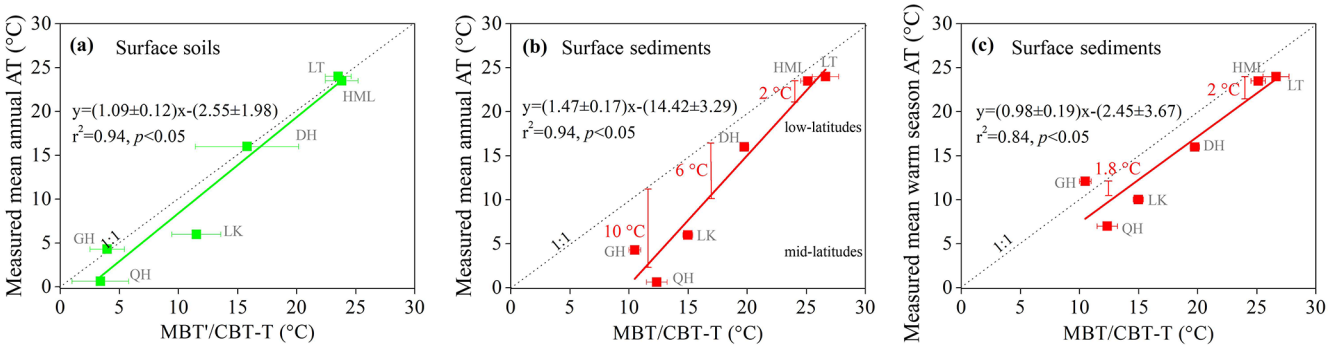

Figure 5. Comparison of brGDGT-derived temperature and measured air temperature. **(a)** Measured mean annual AT and estimated temperatures of brGDGTs in surface soils based on soil calibration Eq. (9). **(b)** Measured mean annual AT and estimated temperatures of brGDGTs in surface sediments based on lake calibration Eq. (11). **(c)** Measured mean warm-season AT and estimated temperatures of brGDGTs in surface sediments based on lake calibration using Eq. (11). Data are from Gonghai Lake (GH; Cao et al., 2017), Lower King Pond (LK; Loomis et al., 2014), Lake Huguang (HML; Hu et al., 2015, 2016), Lake Donghu (DH; Qian et al., 2019), Lake Qinghai (QH; Wang et al., 2012) and Lake Towuli (LT; Tierney and Russell, 2009).

community change can be indicated by the community index ($CI = Ia/(Ia + IIa + IIIa)$) in soils, with $CI > 0.64$ indicating warm community cluster and $CI < 0.64$ indicating cold community cluster. Here we applied the CI to lake sediment data, including ours and those available for all 15 brGDGT compounds in literature, mostly from eastern Africa. As shown in Fig. 4b, the putative two community clusters also occur in lake environments, with the Gonghai community belonging to the "cold" cluster. Different from soil data showing that MBT'_{5ME} captures large temperature changes only when the bacterial community shows a strong change in composition (De Jonge et al., 2019), it seems that MBT'_{5ME} changes linearly with LWT, which is less influenced by the bacterial community change (Fig. 4b). However, we note that the test of community change here is rather crude, and further studies on the biological sources of brGDGTs and their responses to temperature in aquatic environments are needed.

4.4 Ice cover formation as a mechanism for the apparent warm bias of lacustrine brGDGT-derived temperature

One explanation for the warm-season biases of the lacustrine brGDGT-derived temperature in middle to high latitudes has been proposed as the excessive production of brGDGTs during the warm (summer) season relative to the winter season (Pearson et al., 2011; Shanahan et al., 2013; Peterse et al., 2014; Foster et al., 2016; Dang et al., 2018). In Gonghai Lake, the average concentration of brGDGTs in SPM is $7.1 \pm 2.0\,\mathrm{ng\,L^{-1}}$ in September and $5.2 \pm 2.3\,\mathrm{ng\,L^{-1}}$ in January (Fig. 2) with no significant difference. Besides, the compound IIIa″, which is likely specifically of aquatic origin (Weber et al., 2015), also showed no significant seasonal difference ($0.36 \pm 0.09\,\mathrm{ng\,L^{-1}}$ in September vs. $0.31 \pm 0.15\,\mathrm{ng\,L^{-1}}$ in January). More importantly, the small differences in MBT'_{5ME} and MBT'_{6ME} of SPM and their derived temperatures between September and January suggest that the actual seasonal temperature difference, which may be recorded by the immediately produced brGDGTs, would have been substantially masked or smoothed by the predominance of fossil brGDGTs. In addition, brGDGT-derived temperatures in SPM were close to mean annual LWT and lower than the mean warm-season LWT, which also did not support the excessive production of brGDGTs during the warm (summer) season relative to the winter season. Besides, the season of higher brGDGT concentration has been found to be different in different lakes, e.g., in spring and autumn in Lower King Pond (Loomis et al., 2014), in winter in Lake Lucerne (Blaga et al., 2011), and in summer in Lake Donghu in central China (Qian et al., 2019). However, in all of these lakes in temperate climate zones, the brGDGT-derived temperatures have been found to be slightly or significantly warm-season-biased (Loomis et al., 2014; Qian et al., 2019; Fig. 5b). The above evidence suggests that factors other than seasonality in the production of brGDGTs in the lakes could be responsible for the bias of brGDGT-inferred temperature toward warm season in higher latitudes (Fig. 5b and c).

The brGDGT-derived temperature in lake sediments could be influenced by the vertically inhomogeneous production of brGDGTs with a maximum in deep or bottom waters. This seems true in Gonghai Lake, as evidenced by the increase in sedimentary brGDGT content and the decrease in brGDGT-derived temperature with water depth, as discussed above. The bio-precursors of brGDGTs have been proposed to be bacteria with an anaerobic heterotrophic lifestyle (Sinninghe Damsté et al., 2000; Weijers et al., 2006b, 2010; Weber et al., 2015, 2018), implying that a potentially anoxic (micro)environment in deep or bottom water favors the production of brGDGTs (Woltering et al., 2012; Zhang et al., 2016; Weber et al., 2018). Such an occurrence could lead to a higher proportion of "colder-temperature" brGDGTs in lake

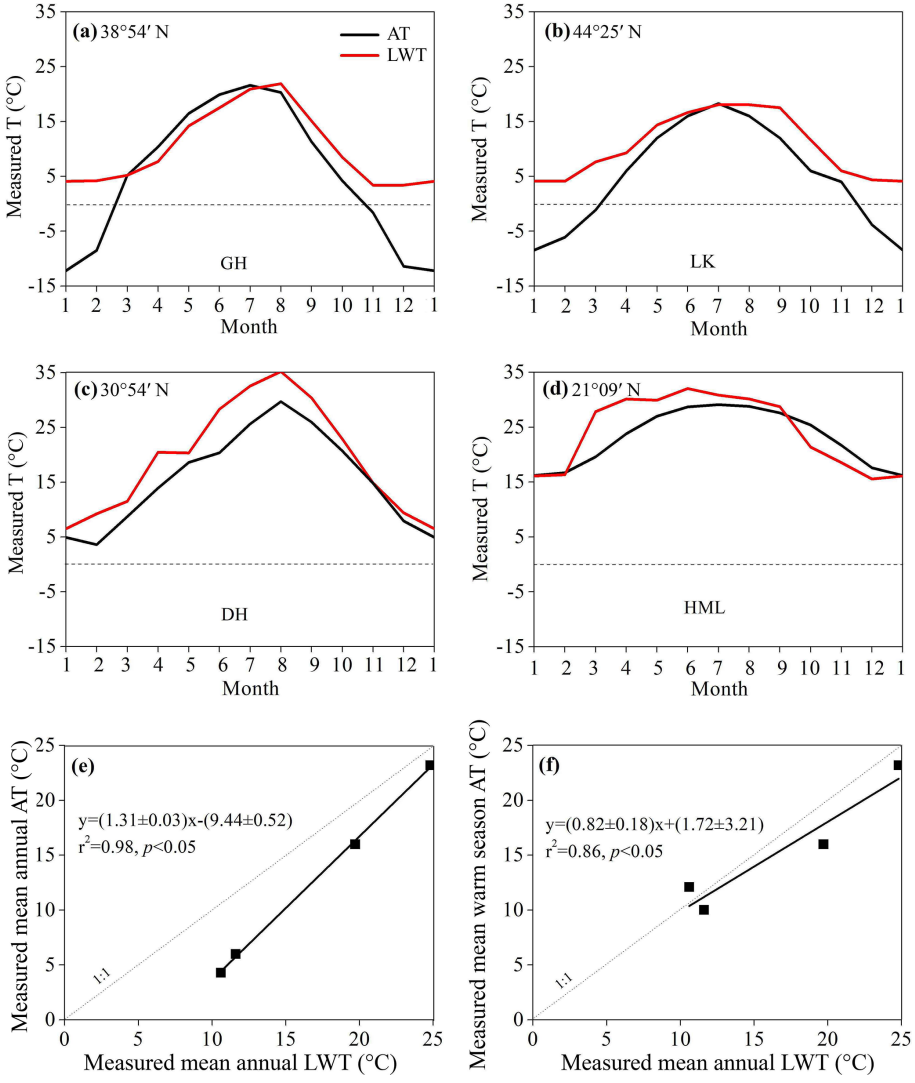

Figure 6. Measured LWT and AT at **(a)** Gonghai Lake (GH; this study), **(b)** Lower King Pond (LK; modified from Loomis et al., 2014), **(c)** Lake Donghu (DH; modified from Qian et al., 2019) and **(d)** Lake Huguang (HML; modified from Hu et al., 2016). **(e)** Correlation between mean annual AT and mean annual LWT. **(f)** Correlation between mean warm-season AT and mean annual LWT. In the midlatitude Gonghai Lake and Lower King Pond, the surface LWT follows AT only when the AT is above freezing. In the low-latitude Lake Donghu and Lake Huguang, the surface LWT follows AT for the whole year.

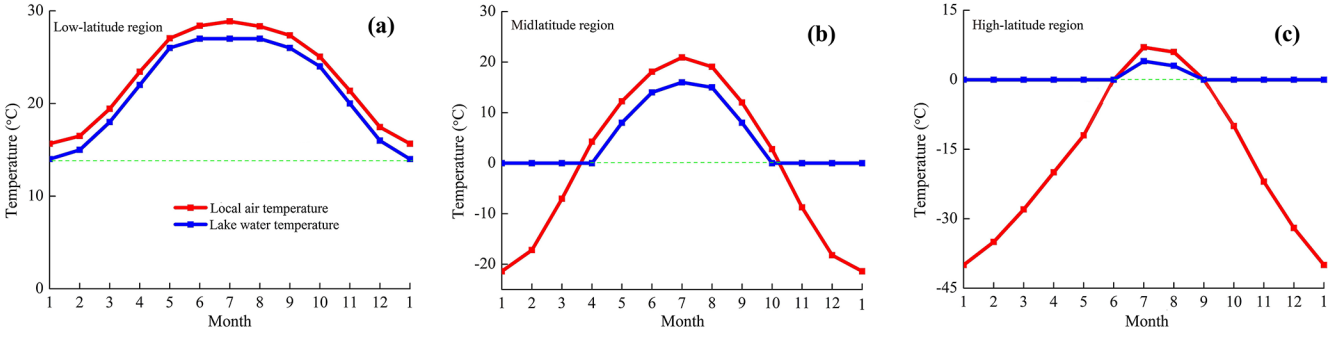

Figure 7. A simple model showing the relationship between LWT and AT in an annual cycle in different latitudes.

sediments, which may at least partly interpret the frequently observed cool bias of brGDGT-derived temperatures in many lakes, such as the Lake Challa, Lake Albert, Lake Edward and Lake Tanganyika (Tierney et al., 2010; Loomis et al., 2012; Buckles et al., 2014a). The MBT–CBT-derived temperature in the tropical Lake Huguang was thought to reflect mean annual AT (Hu et al., 2015, 2016); however, this has recently been proposed as being biased towards winter (cool) values (Chu et al., 2017). We suppose that, as a monomictic lake, the lower mean annual temperature than mean annual AT in deep or bottom waters might be a reason for the cool-biased brGDGT temperature in the lake. Intriguingly, all of the above lakes are in the tropics. Nonetheless, the deep and bottom water bias may be still true for the brGDGT-derived temperature in lakes at higher latitudes, as suggested by our data in Gonghai Lake. However, different from those tropical lakes, in higher-latitude lakes, including Gonghai Lake (this study), Lake Qinghai (Wang et al., 2012), Lower King Pond (Loomis et al., 2014), some cold-region lakes in China (Dang et al., 2018) and some Arctic lakes (Shanahan et al., 2013; Peterse et al., 2014), the sedimentary brGDGT-derived temperatures are all higher, not lower, than the mean annual AT. Therefore, more production of brGDGTs in deep or bottom water alone is not responsible for the warm bias of brGDGT-derived temperature in surface sediments at least in these lakes.

Although brGDGTs in lake sediments were confirmed to be mainly derived from in situ aquatic production, previous studies deemed that the estimated temperatures can still reflect AT by assuming that LWT is tightly coupled with AT (Tierney et al., 2010). In fact, such tight coupling can be found in tropical–subtropical lakes, where AT is always above the freezing point, but this is not true in higher-latitude lakes, such as Lower King Pond and Gonghai Lake, with a lake surface that freezes in winter (Fig. 6a and b). The reason is that lake surface ice prevents the thermal exchange between water and air, leading to decoupling between LWT (usually $\geq 4\,^{\circ}\mathrm{C}$) and AT ($< 0\,^{\circ}\mathrm{C}$) in winter in cold regions. The decoupling makes mean annual LWT, even at the deep and bottom waters, higher than mean annual AT. Therefore, the greater warm biases of brGDGT-derived temperatures from surface sediments in higher latitudes (Fig. 5b) could be due to the stronger decoupling (e.g., longer freezing time) between LWT and AT. Nevertheless, annual mean LWT appears basically close to the mean AT in the warm season (average monthly temperature $> 0\,^{\circ}\mathrm{C}$) (Fig. 6f), which could be the reason why the brGDGT-inferred temperatures are similar to the mean warm-season AT (Fig. 5c). Due to lack of detailed AT and LWT data in literature, we found it difficult to show more examples than those shown in Fig. 6, especially from even higher latitudes. However, we proposed a simple model for the relationship between LWT and AT in a year cycle (Fig. 7), which may be a universal physical phenomenon in shallow lakes. In the middle- and high-latitude region, we believe the decoupling between AT and LWT caused by ice formation in winter may be applied to explain the observed seasonality of the brGDGT temperature records. For example, the biases of brGDGT-derived temperatures toward summer AT observed extensively in the Arctic and Antarctic lakes (Shanahan et al., 2013; Foster et al., 2016) are compatible with the mechanism that we propose here. Of course, considering the limited data in this study, more investigations are needed to test our viewpoint in future studies.

5 Conclusions

We investigated the brGDGT distribution in catchment soils, surface sediments and water column SPM in September and January in Gonghai Lake in northern China. The lake is characterized by ice formation on its surface and a constant $4\,^{\circ}\mathrm{C}$ condition in the underlying water in winter. The brGDGT distribution in sediments was similar to that in SPM but differed clearly from that in soils, indicating mainly in situ production of brGDGTs in the lake. The brGDGTs in SPM showed little seasonal difference in concentration and $\mathrm{MBT}'_{5\mathrm{ME}}$, likely due to a dominant contribution of fossil brGDGTs caused by, e.g., sediment suspension, which may mask any seasonal signals documented in sedimentary brGDGTs. The increase in brGDGT content and decrease in methylation index with water depth in sediments suggested more contribution of aquatic brGDGTs produced from deep and bottom waters. Based on available lake calibrations, we found that the temperature estimates in surface sediments and SPM of Gonghai Lake were higher than the measured mean annual AT but close to warm-season AT, which cannot be interpreted by more aquatic production of brGDGTs in the warm season and/or in deep and bottom waters. We found that such a warm-biased brGDGT-derived temperature was actually close to the mean annual LWT and therefore proposed that water–air temperature decoupling due to ice formation at the lake surface in winter, which can prevent thermal exchange between lake water and air, may be the cause for the apparent bias toward warm AT of lacustrine brGDGT-derived temperatures. Since the warm AT bias of brGDGT estimates has been observed extensively in middle- and high-latitude shallow lakes, we believe the mechanism proposed here could also be applicable to these lakes.

Data availability. The raw data of this study can be accessed from https://figshare.com/s/a4f324247ecd9d1ac575 (Cao et al., 2020).

Supplement. The supplement related to this article is available online at: https://doi.org/10.5194/bg-17-2521-2020-supplement.

Author contributions. ZR designed the experiments, FS and JC collected the samples, and JC carried the experiments out. JC, GJ and ZR prepared the manuscript with contributions from all co-authors.

Competing interests. The authors declare that they have no conflict of interest.

Acknowledgements. Two anonymous reviewers and the associate editor Marcel van der Meer are thanked for their valuable comments.

Financial support. This research has been supported by the Hunan Provincial Natural Science foundation of China (grant no. 2018JJ1017), the National Natural Science Foundation of China (grant no. 41772373), and the Fundamental Research Funds for the Central Universities of China (grant no. lzujbky-2018-it77).

Review statement. This paper was edited by Marcel van der Meer and reviewed by two anonymous referees.

References

Ajioka, T., Yamamoto, M., and Murase, J.: Branched and isoprenoid glycerol dialkyl glycerol tetraethers in soils and lake/river sediments in Lake Biwa basin and implications for MBT/CBT proxies, Org. Geochem., 73, 70–82, https://doi.org/10.1016/j.orggeochem.2014.05.009, 2014.

Blaga, C. I., Reichart, G. J., Heiri, O., and Sinninghe Damsté, J. S.: Tetraether membrane lipid distributions in water-column particulate matter and sediments: a study of 47 European lakes along a north-south transect, J. Paleolimnol., 41, 523–540, https://doi.org/10.1007/s10933-008-9242-2, 2009.

Blaga, C. I., Reichart, G. J., Schouten, S., Lotter, A. F., Werne, J. P., Kosten, S., Mazzeo, N., Lacerot, G., and Sinninghe Damsté, J. S.: Branched glycerol dialkyl glycerol tetraethers in lake sediments: can they be used as temperature and pH proxies, Org. Geochem., 41, 1225–1234, https://doi.org/10.1016/j.orggeochem.2010.07.002, 2010.

Blaga, C. I., Reichart, G. J., Vissers, E. W., Lotter, A. F., Anselmetti, F. S., and Sinninghe Damsté, J. S.: Seasonal changes in glycerol dialkyl glycerol tetraether concentrations and fluxes in a perialpine lake: Implications for the use of the TEX86 and BIT proxies, Geochim. Cosmochim. Ac., 75, 6416–6428, https://doi.org/10.1016/j.gca.2011.08.016, 2011.

Buckles, L. K., Weijers, J. W. H., Verschuren, D., and Sinninghe Damsté, J. S.: Sources of core and intact branched tetraether membrane lipids in the lacustrine environment: Anatomy of Lake Challa and its catchment, equatorial East Africa, Geochim. Cosmochim. Ac., 140, 106–126, https://doi.org/10.1016/j.gca.2014.04.042, 2014a.

Buckles, L. K., Weijers, J. W. H., Tran, X.-M., Waldron, S., and Sinninghe Damsté, J. S.: Provenance of tetraether membrane lipids in a large temperate lake (Loch Lomond, UK): implications for glycerol dialkyl glycerol tetraether (GDGT)-based palaeothermometry, Biogeosciences, 11, 5539–5563, https://doi.org/10.5194/bg-11-5539-2014, 2014b.

Cao, J. T., Rao, Z. G., Jia, G. D., Xu, Q. H., and Chen, F. H.: A 15 ka pH record from an alpine lake in north China derived from the cyclization ratio index of aquatic brGDGTs and its paleoclimatic significance, Org. Geochem., 109, 31–46, https://doi.org/10.1016/j.orggeochem.2017.02.005, 2017.

Cao, J., Rao, Z., Shi, F., and Jia, G.: Ice formation on lake surface in winter causes warm season bias of lacustrine brGDGT temperature estimates, https://doi.org/10.6084/m9.figshare.11422743, 2020.

Chen, F. H., Yu, Z. C., Yang, M. L., Ito, E., Wang, S. M., Madsen, D. B., Huang, X. Z., Zhao, Y., Sato, T., John, B. B. H., Boomer, I., Chen, J. H., An, C. B., and Wünnemann, B.: Holocene moisture evolution in arid central Asia and its out-of-phase relationship with Asian monsoon history, Quaternary Sci. Rev., 27, 351–364, https://doi.org/10.1016/j.quascirev.2007.10.017, 2008.

Chen, F. H., Liu, J. B., Xu, Q. H., Li, Y. C., Chen, J. H., Wei, H. T., Liu, Q. S., Wang, Z. L., Cao, X. Y., and Zhang, S. R.: Environmental magnetic studies of sediment cores from Gonghai Lake: implications for monsoon evolution in North China during the late glacial and Holocene, J. Paleolimnol., 49, 447–464, https://doi.org/10.1007/s10933-012-9677-3, 2013.

Chen, F. H., Xu, Q. H., Chen, J. H., Birks, H. J. B., Liu, J. B., Zhang, S. R., Jin, L. Y., An, C. B., Telford, R. J., Cao, X. Y., Wang, Z. L., Zhang, X. J., Selvaraj, K., Lu, H. Y., Li, Y. C., Zheng, Z., Wang, H. P., Zhou, A. F., Dong, G. H., Zhang, J. W., Huang, X. Z., Bloemendal, J., and Rao, Z. G.: East Asian summer monsoon precipitation variability since the last deglaciation, Sci. Rep.-UK, 5, 11186, https://doi.org/10.1038/srep11186, 2015.

Chu, G., Sun, Q., Zhu, Q., Shan, Y., Shang, W., Ling, Y., Su, Y., Xie, M., Wang, X., and Liu, J.: The role of the Asian winter monsoon in the rapid propagation of abrupt climate changes during the last deglaciation, Quaternary Sci. Rev., 177, 120–129, https://doi.org/10.1016/j.quascirev.2017.10.014, 2017.

Dang, X. Y., Ding, W. H., Yang, H., Pancost, R. D., Naafs, B. D. A., Xue, J. T., Lin, X., Lu, J. Y., and Xie, S. C.: Different temperature dependence of the bacterial brGDGT isomers in 35 Chinese lake sediments compared to that in soils, Org. Geochem., 119, 72–79, https://doi.org/10.1016/j.orggeochem.2018.02.008, 2018.

De Jonge, C., Hopmans, E. C., Stadnitskaia, A., Rijpstra, W. I. C., Hofland, R., Tegelaar, E., and Sinninghe Damsté, J. S.: Identification of novel penta- and hexamethylated branched glycerol dialkyl glycerol tetraethers in peat using HPLC-MS^2, GC-MS and GC-SMB-MS, Org. Geochem., 54, 78–82, https://doi.org/10.1016/j.orggeochem.2012.10.004, 2013.

De Jonge, C., Hopmans, E. C., Zell, C. I., Kim, J. H., Schouten, S., and Sinninghe Damsté, J. S.: Occurrence and abundance of 6-methyl branched glycerol dialkyl glycerol tetraethers in soils: implications for palaeoclimate reconstruction, Geochim. Cosmochim. Ac., 141, 97–112, https://doi.org/10.1016/j.gca.2014.06.013, 2014.

De Jonge, C., Radujković, D., Sigurdsson, B. D., Weedon, J. T., Janssens, I., and Peterse, F.: Lipid biomarker temperature proxy responds to abrupt shift in the bacterial community composition in geothermally heated soils, Org. Geochem., 137, 103897, https://doi.org/10.1016/j.orggeochem.2019.07.006, 2019.

Deng, L. H., Jia, G. D., Jin, C. F., and Li, S. J.: Warm season bias of branched GDGT temperature estimates causes underestimation of altitudinal lapse rate, Org. Geochem., 96, 11–17, https://doi.org/10.1016/j.orggeochem.2016.03.004, 2016.

Foster, L. C., Pearson, E. J., Juggins, S., Hodgson, D. A., Saunders, K. M., Verleyen, E., and Roberts, S. J.: Development of a regional glycerol dialkyl glycerol tetraether

(GDGT)-temperature calibration for Antarctic and sub-Antarctic lakes, Earth Planet. Sc. Lett., 433, 370–379, https://doi.org/10.1016/j.epsl.2015.11.018, 2016.

Hopmans, E. C., Weijers, J. W. H., Schefuß, E., Herfort, L., Sinninghe Damsté, J. S., and Schouten, S.: A novel proxy for terrestrial organic matter in sediments based on branched and isoprenoid tetraether lipids, Earth Planet. Sc. Lett., 224, 107–116, https://doi.org/10.1016/j.epsl.2004.05.012, 2004.

Hu, J. F., Zhou, H. D., Peng, P. A., Yang, X. P., Spiro, B., Jia, G. D., Wei, G. J., and Ouyang, T. P.: Reconstruction of a paleotemperature record from 0.3–3.7 ka for subtropical South China using lacustrine branched GDGTs from Huguangyan Maar, Paleogeogr. Paleocl., 435, 167–176, https://doi.org/10.1016/j.palaeo.2015.06.014, 2015.

Hu, J. F., Zhou, H. D., Peng, P. A., and Spiro, B.: Seasonal variability in concentrations and fluxes of glycerol dialkyl glycerol tetraethers in Huguangyan Maar Lake, SE China: Implications for the applicability of the MBT-CBT paleotemperature proxy in lacustrine settings, Chem. Geol., 420, 200–212, https://doi.org/10.1016/j.chemgeo.2015.11.008, 2016.

Huguet, C., Hopmans, E. C., Febo-Ayala, W., Thompson, D. H., Sinninghe Damsté, J. S., and Schouten, S.: An improved method to determine the absolute abundance of glycerol dibiphytanyl glycerol tetraether lipids, Org. Geochem., 37, 1036–1041, https://doi.org/10.1016/j.orggeochem.2006.05.008, 2006.

Loomis, S. E., Russell, J. M., and Sinninghe Damsté, J. S.: Distributions of branched GDGTs in soils and lake sediments from western Uganda: implications for a lacustrine paleothermometer, Org. Geochem., 42, 739–751, https://doi.org/10.1016/j.orggeochem.2011.06.004, 2011.

Loomis, S. E., Russell, J. M., Ladd, B., Street-Perrott, F. A., and Sinninghe Damsté, J. S.: Calibration and application of the branched GDGT temperature proxy on East African lake sediments, Earth Planet. Sc. Lett., 357–358, 277–288, https://doi.org/10.1016/j.epsl.2012.09.031, 2012.

Loomis, S. E., Russell, J. M., Heureux, A. M., Andrea, W. J. D., and Sinninghe Damsté, J. S.: Seasonal variability of branched glycerol dialkyl glycerol tetraethers (brGDGTs) in a temperate lake system, Geochim. Cosmochim. Ac., 144, 173–187, https://doi.org/10.1016/j.gca.2014.08.027, 2014.

Lu, H. X., Liu, W. G., Yang, H., Wang, H. Y., Liu, Z. H., Leng, Q., Sun, Y. B., Zhou, W. J., and An, Z. S.: 800-kyr land temperature variations modulated by vegetation changes on Chinese Loess Plateau, Nat. Commun., 10, 1958, https://doi.org/10.1038/s41467-019-09978-1, 2019.

Martin, C., Ménot, G., Thouveny, N., Davtian, N., Andrieu-Ponel, V., Reille, M., and Bard, E.: Impact of human activities and vegetation changes on the tetraether sources in Lake St Front (Massif Central, France), Org. Geochem., 135, 38–52, https://doi.org/10.1016/j.orggeochem.2019.06.005, 2019.

Naeher, S., Peterse, F., Smittenberg, R. H., Niemann, H., Zigah, P. K., and Schubert, C. J.: Sources of glycerol dialkyl glycerol tetraethers (GDGTs) in catchment soils, water column and sediments of Lake Rotsee (Switzerland)-implications for the application of GDGT-based proxies for lakes, Org. Geochem., 66, 164–173, https://doi.org/10.1016/j.orggeochem.2013.10.017, 2014.

Naafs, B. D. A., Gallego-Sala, A. V., Inglis, G. N., and Pancost, R. D.: Refining the global branched glycerol dialkyl glycerol tetraether (brGDGT) soil temperature calibration, Org. Geochem., 106, 48–56, https://doi.org/10.1016/j.orggeochem.2017.01.009, 2017.

Niemann, H., Stadnitskaia, A., Wirth, S. B., Gilli, A., Anselmetti, F. S., Sinninghe Damsté, J. S., Schouten, S., Hopmans, E. C., and Lehmann, M. F.: Bacterial GDGTs in Holocene sediments and catchment soils of a high Alpine lake: application of the MBT/CBT-paleothermometer, Clim. Past, 8, 889–906, https://doi.org/10.5194/cp-8-889-2012, 2012.

Pearson, E. J., Juggins, S., Talbot, H. M., Weckström, Jan., Rosén, P., Ryves, D. B., Roberts, S. J., and Schmidt, R.: A lacustrine GDGT-temperature calibration from the Scandinavian Arctic to Antarctic: renewed potential for the application of GDGT-paleothermometry in lakes, Geochim. Cosmochim. Ac., 75, 6225–6238, https://doi.org/10.1016/j.gca.2011.07.042, 2011.

Peterse, F., van der Meer, J., Schouten, S., Weijers, J. W. H., Fierer, N., Jackson, R. B., Kim, J. M., and Sinninghe Damsté, J. S.: Revised calibration of the MBT-CBT paleotemperature proxy based on branched tetraether membrane lipids in surface soils, Geochim. Cosmochim. Ac., 96, 215–229, https://doi.org/10.1016/j.gca.2012.08.011, 2012.

Peterse, F., Vonk, J. E., Holmes, R. M., Giosan, L., Zimov, N., and Eglinton, T. I.: Branched glycerol dialkyl glycerol tetraethers in Arctic lake sediments: sources and implications for paleothermometry at high latitudes, J. Geophys. Res.-Biogeo., 119, 1738–1754, https://doi.org/10.1002/2014jg002639, 2014.

Qian, S., Yang, H., Dong, C. H., Wang, Y. B., Wu, J., Pei, H. Y., Dang, X. Y., Lu, J. Y., Zhao, S. J., and Xie, S. C.: Rapid response of fossil tetraether lipids in lake sediments to seasonal environmental variables in a shallow lake in central China: Implications for the use of tetraether-based proxies, Org. Geochem., 128, 108–121, https://doi.org/10.1016/j.orggeochem.2018.12.007, 2019.

Rao, Z. G., Jia, G. D., Li, Y. X., Chen, J. H., Xu, Q. H., and Chen, F. H.: Asynchronous evolution of the isotopic composition and amount of precipitation in north China during the Holocene revealed by a record of compound-specific carbon and hydrogen isotopes of long-chain *n*-alkanes from an alpine lake, Earth Planet. Sc. Lett., 446, 68–76, https://doi.org/10.1016/j.epsl.2016.04.027, 2016.

Russell, J. M., Hopmans, E. C., Loomis, S. E., Liang, J., and Sinninghe Damsté, J. S.: Distributions of 5- and 6-methyl branched glycerol dialkyl glycerol tetraethers (brGDGTs) in East African lake sediment: Effects of temperature, pH, and new lacustrine paleotemperature calibrations, Org. Geochem., 117, 56–69, https://doi.org/10.1016/j.orggeochem.2017.12.003, 2018.

Schoon, P. L., de Kluijver, A., Middelburg, J. J., Downing, J. A., Sinninghe Damsté, J. S., and Schouten, S.: Influence of lake water pH and alkalinity on the distribution of core and intact polar branched glycerol dialkyl glycerol tetraethers (GDGTs) in lakes, Org. Geochem., 60, 72–82, https://doi.org/10.1016/j.orggeochem.2013.04.015, 2013.

Schouten, S., Hopmans, E. C., and Sinninghe Damsté, J. S.: The organic geochemistry of glycerol dialkyl glycerol tetraether lipids: a review, Org. Geochem., 54, 19–61, https://doi.org/10.1016/j.orggeochem.2012.09.006, 2013.

Shanahan, T. M., Hughen, K. A., and Van Mooy, B. A. S.: Temperature sensitivity of branched and isoprenoid GDGTs in Arctic lakes, Org. Geochem., 64, 119–128, https://doi.org/10.1016/j.orggeochem.2013.09.010, 2013.

Shen, Z. W., Liu, J. B., Xie, C. L., Zhang, X. S., and Chen, F. H.: An environmental perturbation at AD 600 and subsequent human impacts recorded by multi-proxy records from the sediments of Lake Mayinghai, North China, Holocene, 28, 1870–1880, https://doi.org/10.1177/0959683618798159, 2018.

Sinninghe Damsté, J. S.: Spatial heterogeneity of sources of branched tetraethers in shelf systems: The geochemistry of tetraethers in the Berau River delta (Kalimantan, Indonesia), Geochim. Cosmochim. Ac., 186, 13–31, https://doi.org/10.1016/j.gca.2016.04.033, 2016.

Sinninghe Damsté, J. S., Hopmans, E. C., and Pancost, R. D.: Newly discovered non-isoprenoid glycerol dialkyl glycerol tetraether lipids in sediments, Chem. Commun., 23, 1683–1684, https://doi.org/10.1039/b004517i, 2000.

Sun, Q., Chu, G. Q., Liu, M. M., Xie, M. M., Li, S. Q., Ling, Y., Wang, X. H., Shi, L. M., Jia, G. D., and Lü, H. Y.: Distributions and temperature dependence of branched glycerol dialkyl glycerol tetraethers in recent lacustrine sediments from China and Nepal, J. Geophys. Res., 116, G01008, https://doi.org/10.1029/2010jg001365, 2011.

Tierney, J. E. and Russell, J. M.: Distributions of branched GDGTs in a tropical lake system: implications for lacustrine application of the MBT/CBT paleoproxy, Org. Geochem., 40, 1032–1036, https://doi.org/10.1016/j.orggeochem.2009.04.014, 2009.

Tierney, J. E., Russell, J. M., Eggermont, H., Hopmans, E. C., Verschuren, D., and Sinninghe Damsté, J. S.: Environmental controls on branched tetraether lipid distributions in tropical East African lake sediments, Geochim. Cosmochim. Ac., 74, 4902–4918, https://doi.org/10.1016/j.gca.2010.06.002, 2010.

Tierney, J. E., Schouten, S., Pitcher, A., Hopmans, E. C., and Sinninghe Damsté, J. S.: Core and intact polar glycerol dialkyl glycerol tetraethers (GDGTs) in Sand Pond, Warwick, Rhode Island (USA): insights into the origin of lacustrine GDGTs, Geochim. Cosmochim. Ac., 77, 561–581, https://doi.org/10.1016/j.gca.2011.10.018, 2012.

Wang, H. Y., Liu, W. G., Zhang, C. L., Wang, Z., Wang, J. X., Liu, Z. H., and Dong, H. L.: Distribution of glycerol dialkyl glycerol tetraethers in surface sediments of Lake Qinghai and surrounding soil, Org. Geochem., 47, 78–87, https://doi.org/10.1016/j.orggeochem.2012.03.008, 2012.

Wang, H. Y., Liu, W. G., and Lu, H. X.: Appraisal of branched glycerol dialkyl glycerol tetraether-based indices for North China, Org. Geochem., 98, 118–130, https://doi.org/10.1016/j.orggeochem.2016.05.013, 2016.

Wang, M. Y., Zheng, Z., Zong, Y. Q., and Tian, L. P.: Distributions of soil branched glycerol dialkyl glycerol tetraethers from different climate regions of China, Sci Rep.-UK, 9, 2761, https://doi.org/10.1038/s41598-019-39147-9, 2019.

Weber, Y., De Jonge, C., Rijpstra, W. I. C., Hopmans, E. C., Stadnitskaia, A., Schubert, C. J., Lehmann, M. F., Sinninghe Damsté, J. S., and Niemann, H.: Identification and carbon isotope composition of a novel branched GDGT isomer in lake sediments: evidence for lacustrine branched GDGT production, Geochim. Cosmochim. Ac., 154, 118–129, https://doi.org/10.1016/j.gca.2015.01.032, 2015.

Weber, Y., Sinninghe Damsté, J. S., Zopfi, J., De Jonge, C., Gilli, A., Schubert, C. J., Lepori, F., Lehmann, M. F., and Niemann, H.: Redox-dependent niche differentiation provides evidence for multiple bacterial sources of glycerol tetraether lipids in lakes, P. Natl. Acad. Sci. USA, 115, 10926–10931, https://doi.org/10.1073/pnas.1805186115, 2018.

Weijers, J. W. H., Schouten, S., Spaargaren, O. C., and Sinninghe Damsté, J. S.: Occurrence and distribution of tetraether membrane lipids in soils: Implications for the use of the TEX86 proxy and the BIT index, Org. Geochem., 37, 1680–1693, https://doi.org/10.1016/j.orggeochem.2006.07.018, 2006a.

Weijers, J. W. H., Schouten, S., Hopmans, E. C., Geenevasen, J. A. J., David, O. R. P., Coleman, J. M., Pancost, R. D., and Sinninghe Damsté, J. S.: Membrane lipids of mesophilic anaerobic bacteria thriving in peats have typical archaeal traits, Environ. Microbiol., 8, 648–657, https://doi.org/10.1111/j.1462-2920.2005.00941.x, 2006b.

Weijers, J. W. H., Schouten, S., Van den Donker, J. C., Hopmans, E. C., and Sinninghe Damsté, J. S.: Environmental controls on bacterial tetraether membrane lipid distribution in soils, Geochim. Cosmochim. Ac., 71, 703–713, https://doi.org/10.1016/j.gca.2006.10.003, 2007a.

Weijers, J. W. H., Schefuß, N., Schouten, S., and Sinninghe Damsté, J. S.: Coupled thermal and hydrological evolution of tropical Africa over the last deglaciation, Science, 315, 1701–1704, https://doi.org/10.1126/science.1138131, 2007b.

Weijers, J. W. H., Wiesenberg, G. L. B., Bol, R., Hopmans, E. C., and Pancost, R. D.: Carbon isotopic composition of branched tetraether membrane lipids in soils suggest a rapid turnover and a heterotrophic life style of their source organism(s), Biogeosciences, 7, 2959–2973, https://doi.org/10.5194/bg-7-2959-2010, 2010.

Woltering, M., Werne, J. P., Kish, J. L., Hicks, R., Sinninghe Damsté, J. S., and Schouten, S.: Vertical and temporal variability in concentration and distribution of thaumarchaeotal tetraether lipids in Lake Superior and the implications for the application of the TEX86 temperature proxy, Geochim. Cosmochim. Ac., 87, 136–153, https://doi.org/10.1016/j.gca.2012.03.024, 2012.

Xiao, W., Wang, Y., Zhou, S., Hu, L., Yang, H., and Xu, Y.: Ubiquitous production of branched glycerol dialkyl glycerol tetraethers (brGDGTs) in global marine environments: a new source indicator for brGDGTs, Biogeosciences, 13, 5883–5894, https://doi.org/10.5194/bg-13-5883-2016, 2016.

Yang, H., Lü, X. X., Ding, W. H., Lei, Y. Y., Dang, X. Y., and Xie, S. C.: The 6-methyl branched tetraethers significantly affect the performance of the methylation index (MBT') in soils from an altitudinal transect at Mount Shennongjia, Org. Geochem., 82, 42–53, https://doi.org/10.1016/j.orggeochem.2015.02.003, 2015.

Zhang, J., Yu, Z. G., and Jia, G. D.: Cyclisation degree of tetramethylated brGDGTs in marine environments and its implication for source identification, Global Planet. Change, 184, 103043, https://doi.org/10.1016/j.gloplacha.2019.103043, 2020.

Zhang, Z. H., Smittenberg, R. H., and Bradley, R. S.: GDGT distribution in a stratified lake and implications for the application of TEX86 in paleoenvironmental reconstructions, Sci. Rep.-UK, 6, 34465, https://doi.org/10.1038/srep34465, 2016.